



# Interpretable Multimodal Emotion Recognition using Hybrid Fusion of Speech and Image Data

Puneet Kumar<sup>a,2,\*\*</sup>, Sarthak Malik<sup>b,2</sup>, Balasubramanian Raman<sup>a</sup>

<sup>a</sup>Computer Science & Engineering Department, Indian Institute of Technology, Roorkee, 247667, India

<sup>b</sup>Electrical Engineering Department, Indian Institute of Technology, Roorkee, 247667, India

Article history:

Affective Computing, Multimodal Analysis, Speech Processing, Image Processing, Information Fusion.

## ABSTRACT

This paper proposes a multimodal emotion recognition system based on hybrid fusion that classifies the emotions depicted by speech utterances and corresponding images into discrete classes. A new interpretability technique has been developed to identify the important speech & image features leading to the prediction of particular emotion classes. The proposed system's architecture has been determined through intensive ablation studies. It fuses the speech & image features and then combines speech, image, and intermediate fusion outputs. The proposed interpretability technique incorporates the divide & conquer approach to compute shapely values denoting each speech & image feature's importance. We have also constructed a large-scale dataset (IIT-R SIER dataset), consisting of speech utterances, corresponding images, and class labels, i.e., 'anger,' 'happy,' 'hate,' and 'sad.' The proposed system has achieved 83.29% accuracy for emotion recognition. The enhanced performance of the proposed system advocates the importance of utilizing complementary information from multiple modalities for emotion recognition.

© 2022 Elsevier Ltd. All rights reserved.

## 1. Introduction

The multimedia data has overgrown in the last few years, leading multimodal emotion analysis to emerge as an important research trend [1]. Research in this direction aims to help machines become empathetic as emotion analysis is used in various applications such as cognitive psychology, automated identification, intelligent devices, and human-machine interface [2]. Humans portray different emotions through various modalities, among which speech and image are known to contain the human emotions and intentions most effectively [3]. Combining complementary information from both of these modalities could increase emotion recognition accuracy [4].

Researchers have attempted to identify emotions by processing audio and visual information separately [5, 6, 7]. However, multimodal emotion recognition, where the emotional context from multiple modalities are analyzed together, performs better

than the unimodal emotion recognition [4]. In this context, multimodal emotion recognition from speech & text modalities and image & text modalities have been performed; however, emotion recognition from speech & image modalities has not been fully explored. Moreover, most of the existing multimodal approaches do not focus on interpreting the internal working of their emotion recognition systems. It inspired us to develop a multimodal emotion recognition system capable of recognizing emotions portrayed by speech utterances & corresponding images and explaining the importance of each speech segment & visual feature towards emotion recognition.

Multimodal emotion recognition also faces the issue of the unavailability of sufficient labeled datasets for training. Moreover, the real-life multimodal data contains generic images with facial, human, and non-human objects, but most of the existing multimodal datasets contain only facial and human images [8]. A few multimodal datasets are available that contain generic images; however, they consist of positive, negative, and neutral sentiment labels and do not contain multi-class emotion labels [9, 10]. A new dataset, 'IIT Roorkee Speech & Image Emotion Recognition (IIT-R SIER) dataset,' has been

\*\*Corresponding Author

e-mail: [pkumar99@cs.iitr.ac.in](mailto:pkumar99@cs.iitr.ac.in) (Puneet Kumar)

<sup>2</sup>Denotes Equal Contribution

constructed to address this issue. It contains generic images, corresponding speech utterances, and discrete class labels, i.e., ‘anger,’ ‘happy,’ ‘hate,’ and ‘sad.’

The proposed system, ‘ParallelNet,’ recognizes emotions in speech utterances and corresponding images. It implements two networks,  $N1$  and  $N2$ , to fuse the information of speech and image modalities in a hybrid manner of intermediate and late fusion. The architectures for  $N1$  and  $N2$  are determined through extensive ablation studies. A technique to interpret the important input features and predictions has also been developed. The proposed system has performed with an accuracy of 83.29% on the IIT-R SIER dataset. The dataset and code for this paper are accessible at [github.com/MIntelligence-Group/SpeechImg\\_EmoRec](https://github.com/MIntelligence-Group/SpeechImg_EmoRec).

The paper makes the following major contributions.

- A hybrid-fusion-based novel system, ‘ParallelNet,’ has been proposed to classify an input containing speech utterance & corresponding image into discrete emotion classes. It combines the information from speech & image modalities using a hybrid of intermediate and late fusion.
- A large-scale dataset, ‘IIT-R SIER dataset’ containing speech utterances, corresponding images, and emotion labels, has been constructed.
- A new interpretability technique has been developed to identify the important parts of the input speech and image that contribute the most to recognizing emotions.

Further in this paper, the related works have been reviewed in Section 2. The proposed dataset, system, and interpretability technique have been described in Section 3 along with the dataset construction procedure. Section 4 and 5 discuss the experiments and results and the paper is concluded in Section 6.

## 2. Related works

This Section surveys the existing literature on speech & image emotion recognition and deep neural network interpretability.

### 2.1. Speech emotion recognition

The deep learning-based approaches using spectrogram features and attention mechanisms have shown state-of-the-art results for speech emotion recognition (SER) [11, 12, 13]. In this context, Xu et al. [5] generated multiple attention maps, fused and used them for SER. They observed an increased performance as compared to non-fusion-based approaches. In another work, Majumder et al. [6] implemented a deep neural network to track speakers’ identities showing specific emotions.

### 2.2. Image emotion recognition

Image Emotion Recognition (IER) research is also an active domain. For instance, Kim et al. [3] built a deep feed-forward neural network to combine different levels of emotion features obtained by using the semantic information of the image. In another work, Rao et al. [7] prepared hierarchical notations for emotion recognition in the visual domain.

Humans portray emotions through multiple modalities, among which speech and image modalities contain the human

emotions and intentions most effectively [3]. Analysis in a single modality may not be able to recognize the emotional context completely, which leads to the need for multimodal emotion recognition approaches that analyze multimodal audio-visual emotional context [4].

### 2.3. Multimodal emotion recognition

Multimodal emotion analysis from audio-visual data has started getting researchers’ attention lately [14, 15, 16]. For instance, Siriwardhana et al. [17] fine-tuned Transformers-based models to improve the performance of multimodal speech emotion recognition. Multimodal emotion recognition has been carried out for text & speech modalities [18, 19] and text & image modalities [10, 9, 15]. However, it has not been fully explored for speech & image modalities. Moreover, most deep learning-based multimodal emotion recognition systems work as a black box where it is challenging to interpret their internal working. It inspired us to develop an interpretable multimodal emotion recognition system for speech & image modalities.

### 2.4. Interpretability of deep neural networks

The existing interpretability approaches compute each input feature’s importance by backpropagating the network or observing the changes in output on changing the input [20]. In this direction, Riberio et al. [21] developed a framework to explain a classifier’s predictions by determining the approximated importance of each input. Researchers have explained the layer-by-layer learning of deep neural networks, traced the contributions of all the neurons, and understood the output by breaking it down into parts [19, 22]. There are interpretability methods for visual analysis to compute input pixels’ importance [20, 21, 23]. However, such methods have not been sufficiently explored for speech modality. It inspired us to develop an interpretability technique for multimodal emotion recognition to explain the importance of each speech segment and each visual feature of the input.

## 3. Materials and methods

### 3.1. Dataset construction

The ‘IIT Roorkee Speech & Image Emotion Recognition (IIT-R SIER) dataset has been constructed using Balanced Twitter for Sentiment Analysis (B-T4SA) dataset [10]. The recent text-to-speech models are known to generate high-quality audio that can be used as a valid approximation of natural audio signals [24, 25, 26]. A pre-trained state-of-the-art text-to-speech model, DeepSpeech3 [24] has been used to convert the text from the B-T4SA dataset to speech. The samples are manually cleaned by removing the corrupt and duplicate samples. Further, the following procedure has been followed to generate the ground-truth labels according to the overall emotional context represented by both modalities in combination.

The speech component of each data sample is passed through the SER model trained on IEMOCAP [8] dataset; classification probabilities for each emotion class are obtained, and the maximum among the probabilities for all emotion classes is noted as  $max_1$ . Likewise, each sample’s image component is passed

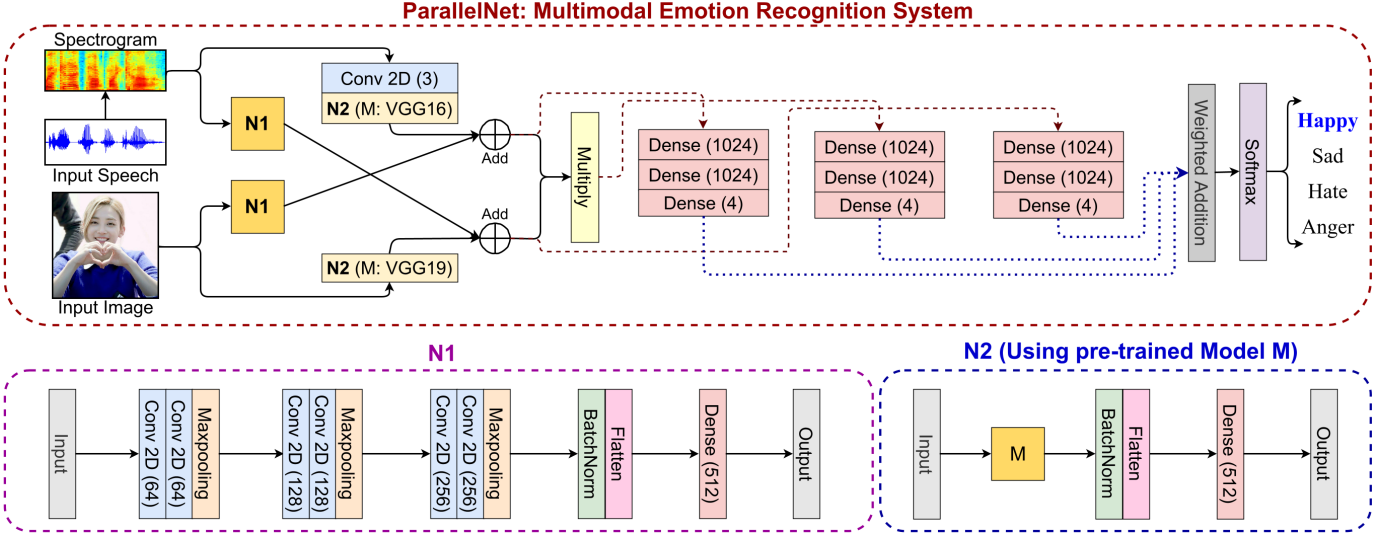


Fig. 1: Architecture of the proposed system (top),  $N1$  (bottom left) and  $N2$  (bottom right) where  $M$  is a pre-trained model.

through the IER model trained on Flickr & Instagram (FI) [27] dataset and the maximum of classification probabilities for all emotion classes, i.e.,  $max_2$  is noted. The higher of  $max_1$  and  $max_2$  is observed, and the corresponding emotion label is assigned as the ground-truth label to the data sample. For example, if IER model returned probabilities 0.1, 0.8, 0.05 and 0.05 for four emotion classes while SER model gave 0.1, 0.1, 0.7 & 0.1 then we assigned second emotion class to the sample considering  $max(0.8 \text{ and } 0.7)$ . The samples having  $max(max_1, max_2)$  less than a threshold of 0.5 are discarded as the predicted class label must be at least double confident than random prediction (probability 0.25). The samples labeled as ‘excitement’ & ‘disgust’ have been re-labeled as ‘happy’ & ‘hate’ as per Plutchik’s wheel of emotions [28]. The final dataset contains a total of 80,893 samples with 42,958 labeled as ‘happy,’ 13621 as ‘sad’ and 4401 & 19,913 as ‘hate’ and ‘anger’ respectively.

### 3.2. Proposed multimodal emotion recognition system

Fig. 1 depicts the architecture of the proposed multimodal emotion recognition system, which is determined in Section 4.3 through the ablation studies. A hybrid of intermediate and late fusion is implemented where intermediate fusion combines various modalities’ information before classifying, while late fusion fuses the results after classification. The input image is in the space domain. The speech has been converted from the time domain to a log-mel spectrogram, i.e., space domain. The proposed system contains networks  $N1$  and  $N2$  and dense, multiply, weighted addition, and softmax layers.  $N1$  uses convolution & max-pool layers while  $N2$  uses pre-trained networks VGG16 and VGG19 [29]. Both of these networks contain batch-normalization, flatten, and dense layers.

#### 3.2.1. Intermediate fusion phase

Consider the networks fed with the image input to be  $N1_i$  and  $N2_i$  while the networks  $N1_s$  and  $N2_s$  process the speech input. The speech is expressed as a spectrogram of size (128, 128, 1) and passed first to a convolution layer having three convolutional filters of size (1, 1) each and then to  $N2_s$  where a

pre-trained VGG16 network is used. The image with size (128, 128, 3) is passed to  $N2_i$  that uses a pre-trained VGG19 network. As shown in Eq. 1, the output of  $N1_s$  is added with the output of  $N2_i$  to get  $F_s$ . Likewise, the outputs of  $N1_i$  and  $N2_s$  are added to obtain  $F_i$ . Then  $F_s$  and  $F_i$  are element-wise multiplied to obtain  $F_{mul}$ .

$$\begin{aligned} F_i &= Add(output(N1_i), output(N2_s)) \\ F_s &= Add(output(N1_s), output(N2_i)) \\ F_{mul} &= Multiply(F_i, F_s) \end{aligned} \quad (1)$$

The choice of using multiplication instead of weighted addition in Eq. 1 to combine  $F_s$  and  $F_i$  in the low-level fusion has been determined experimentally. Moreover, theoretically, if the speech and image modalities predict the same emotion class, they should support each other. However, let’s consider a case where one modality predicts  $i^{th}$  emotion very strongly while another predicts another emotion  $j^{th}$  weakly. We expect that the  $i^{th}$  emotion should be predicted weakly. It would not have been the case in the case of using addition, and the  $i^{th}$  emotion would have the upper hand. In comparison, multiplication of both the modalities would dilute the assertive behavior of the  $i^{th}$  emotion and give us the expected prediction.

#### 3.2.2. Late fusion phase

The intermediate outputs  $F_i$ ,  $F_s$ , and  $F_{mul}$  are passed from three dense layers of size 1024, 1024, and 4 to obtain  $O_{sp}$  for speech,  $O_{img}$  for image, and  $O_{mul}$  for multiplied. These outputs are combined using the weighted addition layer as per Eq. 2 in a late fusion manner and passed from a softmax layer to get the final predicted label,  $\hat{y}$ . The weights  $w_1$ ,  $w_2$ , and  $w_3$  are randomly initialized and passed to a softmax layer to normalize them to non-negative values. Their final values are learned using the Gradient Descent algorithm. It combines the information from speech & image modalities and the output of intermediate fusion in a hybrid manner.

$$\begin{aligned} O &= w_1 \times O_{sp} + w_2 \times O_{img} + w_3 \times O_{mul} \\ \hat{y} &= Softmax(O) \end{aligned} \quad (2)$$

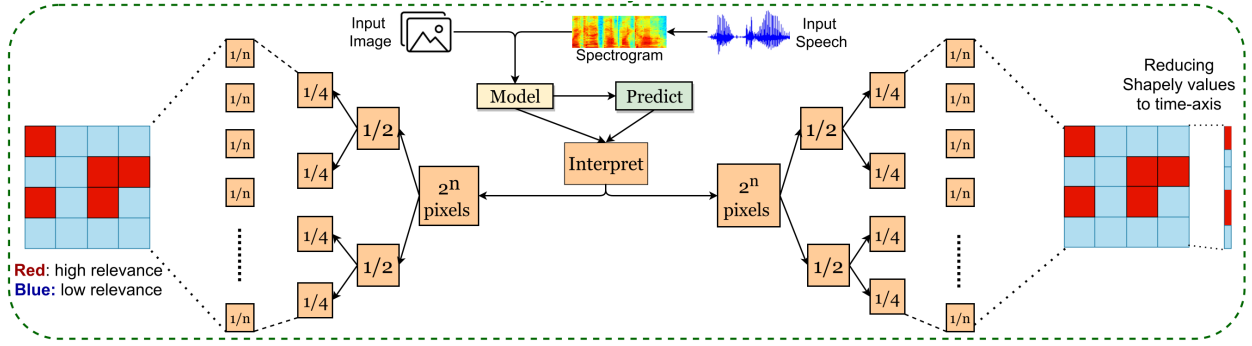


Fig. 2: Proposed interpretability technique’s illustration. Here, each part’s importance is computed using Divide & Conquer.

### 3.3. Proposed interpretability technique

While making predictions, a deep learning-based classifier is expected to consider the input features that a human would consider. However, it is challenging to look into it and understand what input features it is considering [21]. To work on this challenge, we have developed an interpretability technique based on ‘shapely values’ [20] that denotes each input feature’s importance. Theoretically, shapely values’ computation takes exponential time. As depicted in Eq. 3, the divide and conquer approach has been used to approximate the computation. For a model with two features  $f_1$  and  $f_2$ , shapely value  $S_{\{f_1\}}$  for feature  $f_1$  denoting its importance is computed as follows.

$$S_{\{f_1\}} = (1/2) \times MC_{f_1, \{f_1\}} + (1/2) \times MC_{f_1, \{f_1, f_2\}} \quad (3)$$

Here,  $MC_{f_1, \{f_1\}}$  is feature  $f_1$ ’s marginal contribution to the model containing only  $f_1$  and given by Eq. 4 where  $score_{\{f_1\}}$  denotes the prediction for the ground-truth label using the model with feature  $f_1$ .

$$MC_{f_1, \{f_1\}} = score_{\{f_1\}} - score_{\{\phi\}} \quad (4)$$

The respective speech and image inputs are segregated and fed into the model while keeping the other as zero to compute the individual contribution of each modality. As depicted in Fig. 2, each modality’s input is divided into two parts for a specified number of times, and the importance of each part towards the model’s prediction is computed as per Eq. 2. Moreover, the calculation of the importance score follows the basic requirement of shapely values given by Eq. 5.

$$S_{\{f_1\}} + S_{\{f_2\}} = S_{\{f_1, f_2\}} - S_{\{null\}} \quad (5)$$

The important image features for the predictions can be directly observed through the shapely values. In contrast, the important speech features are analyzed after transforming it to wave, i.e., time-domain representation. We first applied the shapely values directly and converted the spectrogram to speech; however, the speech reconstructed by this method was not meaningful. Then, we used the method of averaging the shapely values along the frequency axis and reducing them to the time axis to find the features’ importance at a given time. The speech segments below a threshold shapely values of 30 percentile have been reduced to zero. The leftover segment with high importance is converted to text using speech-to-text model [30] and interpreted to understand how the model classifies each instance. The proposed interpretability technique has been summarised in Algorithm 1.

## 4. Experiments

### 4.1. Experimental setup

The network training for the proposed system has been carried out on Nvidia Quadro P5000 GPU, whereas the testing & evaluation have been done on an Intel(R) Core(TM) i7-8700 Ubuntu machine with 64 bit OS and 3.70 GHz, 16GB RAM.

### 4.2. Training strategy

The model training has been performed using a batch-size of 64, train-test split of 70-30, 5-fold cross-validation, *Adam* optimizer, *ReLU* activation function with a learning rate of  $8 \times 10^{-6}$ . The baselines and proposed models converged in terms of validation loss in 18-23 epochs. As a safe upper bound, the models have been trained for 30 epochs. A weighted combination of categorical focal loss [31] and **categorical cross entropy** with weights 1 and 0.5 has been used as the loss function. *EarlyStopping* and *ReduceLROnPlateau* have been incorporated with patience values 5 and 2. Accuracy, macro f1 [32], and *CohenKappa* [33] have been analyzed for evaluation.

### 4.3. Ablation studies and models

The ablation studies have been performed to analyze the effect of combining the information from multiple modalities and using various network configurations.

#### 4.3.1. Effect of multiple modalities

We first worked on SER and IER alone, using only speech samples and images from the IIT-R SIER dataset. Then we combined the information from speech & image modalities and performed multimodal emotion recognition. The IER-only experiments demonstrated high training but low validation accuracy. The convergence of accuracy and f1 score was not in line, and *CohenKappa* metric’s value was low, denoting over-fitting for a particular class. The accuracy and f1 score converged in line for SER-only experiments, though the accuracy was less.

#### 4.3.2. Effect of various network configurations

As depicted in Fig. 1, the proposed system consists of a family of networks where  $N1$  and  $N2$  can be varied in different situations. We first keep  $N2$  fixed as EfficientNet [34] and evaluate three configurations for  $N1$  – Configuration 1 uses two criss-cross before and after  $N2$ . A *criss-cross* is a position combining two different modalities’ networks. Configuration 2 & 3

**Algorithm 1:** Proposed interpretability technique

---

**Result:**  $SHAP\_value\_img$ ,  $SHAP\_value\_speech$   
 Define  $model$  : Multimodal deep neural network;  
 Define  $data\_img$  : Image pixels;  
 Define  $data\_speech$  : speech spectrogram pixels;  
 Define  $wd, ht$  : Width & height;  
 Define  $times$  : Number of division to divide image & speech spectrogram in;  
 Define  $SHAP\_value\_img$  : Image’s shaply value;  
 Define  $SHAP\_value\_speech$  : Speech’s shaply value;  
 Procedure  $DnCSHap\_MM(model, data\_img, data\_speech, wd, ht, times)$

```

  ▶ Initialize data with all zero entries, here; np: numpy
  data_1 = np.zeros([wd, ht, 3]);
  data_2 = np.zeros([wd, ht, 1]);
  data_1 = data_1.reshape(1, wd, ht, 3);
  data_2 = data_2.reshape(1, wd, ht, 1);

  ▶ Make original data ready to be fed into model
  data_f_img = data_img.reshape(1, wd, ht, 3);
  data_f_speech = data_speech.reshape(1, wd, ht, 1);

  ▶ Find the predicted label
  pred = model.predict(data_f_img, data_f_speech);
  arg_max = np.argmax(pred);

  ▶ Find predicted probability with original data
  pred_f = pred[0][arg_max];

  ▶ Find predicted probability with blank data
  pred_b = model.predict(data_1, data_2)[0][arg_max];

  ▶ Find predicted probability with only image modality
  pred_1 = model.predict(data_f_img, data_2)[0][arg_max];

  ▶ Find predicted probability with only speech modality
  pred_2 = model.predict(data_1, data_f_speech)[0][arg_max];

  ▶ Compute the importance of image & speech
  score_1 = ((pred_1 - pred_b) + (pred_f - pred_2))/2;
  score_2 = ((pred_2 - pred_b) + (pred_f - pred_1))/2

  ▶ Placeholders for speech & image shap values
  SHAP_value_img = np.zeros([wd, ht]);
  SHAP_value_speech = np.zeros([wd, ht]);
  times = times - 1

  ▶ Compute SHAP_value_img and SHAP_value_speech
  Compute SHAP_value_img using Eq. 3, 4 and 5;
  Compute SHAP_value_speech using Eq. 3, 4 and 5
  
```

---

implement single criss-cross before and after  $N2$ . Three baseline models have been implemented in line with these configurations. Configuration 3 was chosen for final implementation as it shows in-line convergence & improved performance.

Further, keeping Configuration 3 fixed for  $N1$ ’s configuration, following choices have been evaluated for  $N2$  – VGG [29] (VGG-16, VGG-19), ResNet [35] (ResNet-34, ResNet-50, ResNet-101), InceptionNet [36] (Inception 3a, Inception 4a), MobileNet [37] and DenseNet [38]. The best performance has been observed with VGG16 as  $N2_s$  and VGG19 as  $N1_i$  which

have finally been implemented by the ‘ParallelNet’. The baseline & proposed models determined through aforementioned studies are listed below and their performance in terms of validation accuracies have been summarized in Table 1.

- **Baseline 1** –  $N1$ : Two criss-cross,  $N2$ : EfficientNet.
- **Baseline 2** –  $N1$ : Criss-cross before  $N2$ ;  $N2$ : EfficientNet.
- **Baseline 3** –  $N1$ : Criss-cross after  $N2$ ;  $N2$ : EfficientNet.
- **Proposed** –  $N1$ : Criss-cross after  $N2$ ;  $N2$ : VGG.

Table 1: Ablation studies’ summary.

Model	Accuracy
SER Only	60.17%
IER Only	66.93%
Baseline 1	63.93%
Baseline 2	61.81%
Baseline 3	67.70%
Proposed (‘ParallelNet’)	<b>83.29%</b>

## 5. Results and discussion

The emotion classification results have been discussed in this Section, along with their interpretation and a comparison of sentiment classification results with existing methods.

### 5.1. Quantitative results

The ‘ParallelNet’ has achieved emotion recognition accuracy of **83.29%**. Its class-wise accuracies are shown in Fig. 3.

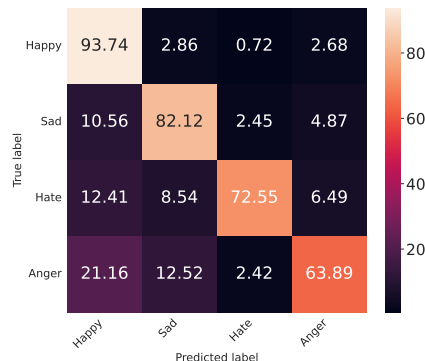


Fig. 3: Confusion matrix showing class-wise accuracies.

### 5.2. Qualitative results

Fig. 4 shows sample emotion classification & interpretation results. The important speech and image features contributing to emotion classification are obtained, and corresponding words are highlighted. In the waveform, yellow and blue correspond to the most and least important features.

### 5.3. Results comparison

The emotion recognition results have been reported in Section 5.1. The IIT-R SIER dataset has been constructed from the B-T4SA dataset in this paper; hence, there are no existing emotion recognition results for it. However, sentiment classification (into neutral, negative, and positive classes) results on the B-T4SA dataset are available in the literature, which have been compared with the proposed method’s sentiment classification results in Table 2.

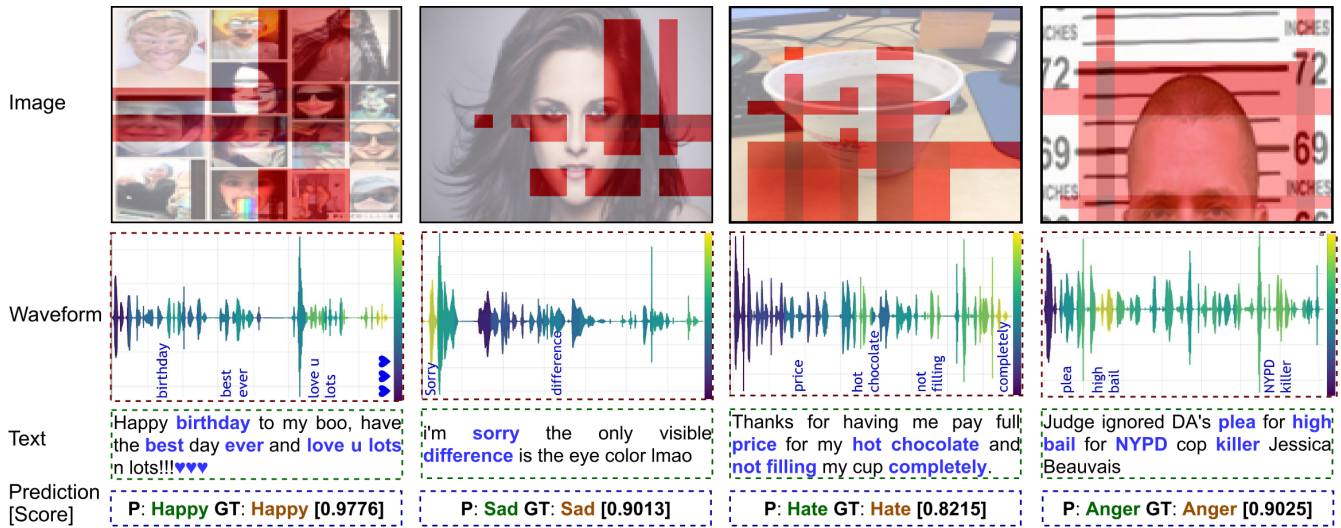


Fig. 4: Sample results; here, ‘P’, ‘GT’ and ‘Score’ denote the predicted label, ground-truth label and softmax score.

Table 2: Comparing existing sentiment analysis results

Approach	Author	Accuracy
Cross-Modal Learning	Vadicamo et al. [10]	51.30%
Multimodal Sentiment Analysis	Gaspar et al. [9]	60.42%
ParallelNet (Proposed)		<b>89.68%</b>

#### 5.4. Discussion

The proposed system classifies a given multimodal input containing speech & corresponding image into ‘anger,’ ‘happy,’ ‘hate,’ and ‘sad’ classes. The proposed interpretability technique identifies the important speech & image features contributing towards emotion recognition. An alternate procedure to construct the ITR-SIER dataset was to retain only those samples from the BT4SA dataset for which SER & IER models predicted the same label and discard the rest of the samples. However, it would have caused a bias towards the models used in the first place for creating these labels. The SER & IER models have been retrained on the ITR-SIER dataset instead of using the pre-trained weights of the models used to construct the ITR-SIER dataset. However, suppose somebody uses the pre-trained models of either one of the two modalities (trained on IEMOCAP and Flickr & Instagram datasets, respectively) used during dataset construction. In that case, they will get a 100% accuracy. The closest to them any other evaluated machine learning model is, the more favorable its evaluation would be. That’s why the proposed procedure of considering the prediction probabilities for all emotion classes is more effective in capturing the overall emotional context represented by both modalities in combination. It leads to generating more accurate ground-truth labels.

The proposed system’s architecture has been determined through extensive ablation studies. It consists of a family of networks where  $N1$  and  $N2$  can be varied in different situations. We’ve first determined the optimal configuration for  $N1$  to combine speech & image modalities’ information. Further, VGG, ResNet, InceptionNet, MobileNet, and DenseNet have been evaluated for  $N2$ . The best performance has been ob-

served with VGG. The ResNet depicted very slow learning for a lower learning rate while the learning fluctuated a lot for a higher learning rate. The model converged faster for the Inception Net and Efficient Net; however, the accuracy is lower. MobileNet and DenseNet have also resulted in low performance.

Apart from the experimental validation in Table 1, Fig. 4 qualitatively re-affirms the importance of combining complementary information from multiple modalities for more accurate emotion recognition. In the first & second cases, the image and speech features (shown by yellow parts of the waveform and denoted by corresponding words in blue) contribute to predicting the emotion class ‘sad.’ In the third & fourth cases, the image features have not been precisely captured, and the images seem neutral. However, the corresponding speech features *not filling* and *killer* contribute towards hatred and anger intent, which leads to the recognition of ‘hate’ and ‘anger’ classes.

## 6. Conclusions and future work

The importance of utilizing the information from multiple modalities has been established for emotion recognition. The proposed system, ‘ParallelNet,’ has resulted in better performance than SER alone, IER alone, and baseline models. The proposed interpretability technique identifies the important speech & image features contributing to emotion recognition. The future research plan includes working on emotion recognition interpretability, including more modalities., i.e., text, videos, and human activity data.

### Declaration of Competing Interest

The authors declare that they have no known competing financial interests or personal relationships that could have appeared to influence the work reported in this paper.

### Acknowledgements

Ministry of Education, India, has supported this work with grant no. 1-3146198040. It has been carried out at the Machine Intelligence Lab, IIT Roorkee, India.

## References

- [1] T. Baltrušaitis, C. Ahuja, L.-P. Morency, Multimodal Machine Learning: A Survey and Taxonomy, *IEEE Transactions on Pattern Analysis and Machine Intelligence (T-PAMI)* 41 (2) (2018) 423–443.
- [2] S. Poria, E. Cambria, R. Bajpai, A. Hussain, A Review of Affective Computing: From Unimodal Analysis to Multimodal Fusion, *Elsevier Information Fusion Journal* 37 (2017) 98–125.
- [3] H.-R. Kim, Y.-S. Kim, S. J. Kim, I.-K. Lee, Building Emotional Machines: Recognizing Image Emotions through Deep Neural Networks, *IEEE Transactions on Multimedia (T-MM)* 20 (11) (2018) 2980–2992.
- [4] Z. Zeng, M. Pantic, G. I. Roisman, T. S. Huang, A Survey of Affect Recognition: Audio, Visual, and Spontaneous Expressions, *IEEE Transactions on Pattern Analysis and Machine Intelligence (T-PAMI)* 31 (1) (2009) 39–58.
- [5] M. Xu, F. Zhang, S. U. Khan, Improve Accuracy of Speech Emotion Recognition with Attention Head Fusion, in: *IEEE Annual Computing and Communication Workshop and Conference (CCWC)*, 2020, pp. 1058–1064.
- [6] N. Majumder, S. Poria, D. Hazarika, R. Mihalcea, A. Gelbukh, E. Cambria, DialogueRNN: An Attentive RNN for Emotion Detection in Conversations, in: *Conference on Artificial Intelligence (AAAI)*, Vol. 33, 2019, pp. 6818–6825.
- [7] T. Rao, X. Li, M. Xu, Learning Multi-level Deep Representations for Image Emotion Classification, *Neural Processing Letters* pp. 1–19 (2019).
- [8] C. Busso, M. Bulut, C.-C. Lee, A. Kazemzadeh, E. Mower, S. Kim, J. N. Chang, S. Lee, S. S. Narayanan, IEMOCAP: Interactive Emotional dyadic MOtion CAPture data, *Language Resources and Evaluation* 42 (4) (2008).
- [9] A. Gaspar, L. A. Alexandre, A Multimodal Approach to Image Sentiment Analysis, in: *Springer International Conference on Intelligent Data Engineering and Automated Learning (IDEAL)*, 2019, pp. 302–309.
- [10] L. Vadicamo, F. Carrara, A. Cimino, S. Cresci, F. Dell’Orletta, F. Falchi, M. Tesconi, Cross-Media Learning for Image Sentiment Analysis in the Wild, in: *IEEE International Conference on Computer Vision Workshops (ICCV-W)*, pp. 308–317.
- [11] D. Dai, Z. Wu, R. Li, X. Wu, J. Jia, H. Meng, Learning Discriminative Features from Spectrograms using Center Loss for SER, in: *IEEE International Conference on Acoustics, Speech and Signal Processing (ICASSP)*, 2019, pp. 7405–7409.
- [12] P. Yenigalla, A. Kumar, S. Tripathi, C. Singh, S. Kar, J. Vepa, Speech Emotion Recognition Using Spectrogram & Phoneme Embedding., in: *INTERSPEECH*, 2018, pp. 3688–3692.
- [13] P. Kumar, S. Jain, B. Raman, P. P. Roy, M. Iwamura, End-to-End Triplet Loss based Emotion Embedding System for Speech Emotion Recognition, in: *IEEE International Conference on Pattern Recognition (ICPR)*, 2021, pp. 8766–8773.
- [14] M. S. Hossain, G. Muhammad, Emotion Recognition using Deep Learning Approach from Audio Visual Emotional Big Data, *Information Fusion* 49 (2019) 69–78.
- [15] P. Kumar, V. Khokher, Y. Gupta, B. Raman, Hybrid Fusion based Approach for Multimodal Emotion Recognition with Insufficient Labeled Data, in: *2021 IEEE International Conference on Image Processing (ICIP)*, IEEE, 2021, pp. 314–318.
- [16] C. Guanghui, Z. Xiaoping, Multimodal Emotion Recognition by Fusing Correlation Features of Speech-Visual, *IEEE Signal Processing Letters* 28 (2021) 533–537.
- [17] S. Siriwardhana, A. Reis, R. Weerasekera, Jointly Fine Tuning ‘BERT-Like’ Self Supervised Models to Improve Multimodal Speech Emotion Recognition, *INTERSPEECH (2020)* 3755–3759.
- [18] M. R. Makiuchi, K. Uto, K. Shinoda, Multimodal Emotion Recognition with High-level Speech and Text Features, in: *IEEE Automatic Speech Recognition and Understanding Workshop (ASRU)*, 2021.
- [19] P. Kumar, V. Kaushik, B. Raman, Towards the Explainability of Multimodal Speech Emotion Recognition, in: *INTERSPEECH*, 2021, pp. 1748–1752.
- [20] S. M. Lundberg, S.-I. Lee, A Unified Approach to Interpreting Model Predictions, in: *The 31st International Conference on Neural Information Processing Systems (NeurIPS)*, 2017, pp. 4768–4777.
- [21] M. T. Ribeiro, S. Singh, C. Guestrin, Why Should I Trust You? Explaining Predictions of Any Classifier, in: *International Conference on Knowledge Discovery & Data Mining (KDD)*, 2016, pp. 1135–1144.
- [22] A. Shrikumar, P. Greenside, A. Kundaje, Learning Important Features Through Propagating Activation Differences, in: *International Conference on Machine Learning (ICML)*, 2017, pp. 3145–3153.
- [23] S. Malik, P. Kumar, B. Raman, Towards Interpretable Facial Emotion Recognition, in: *The 12th Indian Conference on Computer Vision, Graphics and Image Processing (ICVGIP)*, 2021, pp. 1–9.
- [24] W. Ping, K. Peng, A. Gibiansky, S. O. Arik, A. Kannan, S. Narang, J. Raiman, J. Miller, DeepVoice 3: Scaling Text-to-Speech with Convolutional Sequence Learning., in: *The 6th Int. Conference on Learning Representations (ICLR)*, 2018.
- [25] D. Mind, Wavenet: A Generative Model for Raw Audio, [deepmind.com/blog/article/wavenet-generative-model-raw-audio](https://deepmind.com/blog/article/wavenet-generative-model-raw-audio), Accessed on 20.02.2022 (2016).
- [26] A. v. d. Oord, S. Dieleman, H. Zen, K. Simonyan, O. Vinyals, A. Graves, N. Kalchbrenner, A. Senior, K. Kavukcuoglu, Wavenet: A Generative Model for Raw Audio, *arXiv preprint arXiv:1609.03499* (2016).
- [27] Q. You, J. Luo, H. Jin, J. Yang, Building a Large Scale Dataset for Image Emotion Recognition: the Fine Print and the Benchmark, in: *The 30th AAAI Conference on Artificial Intelligence (AAAI)*, 2016, pp. 308–314.
- [28] R. Plutchik, The Nature of Emotions, *Journal Storage Digital Library’s American scientist Journal* 89 (4) (2001) 344–350.
- [29] K. Simonyan, A. Zisserman, Very Deep Convolutional Networks for Large-Scale Image Recognition, *arXiv:1409.1556* Accessed on 30.01.2022 (2014).
- [30] W. Chan, N. Jaitly, Q. Le, O. Vinyals, Listen, Attend and Spell: A Neural Network for Large Vocabulary Conversational Speech Recognition, in: *IEEE International Conference on Acoustics, Speech and Signal Processing (ICASSP)*, 2016, pp. 4960–4964.
- [31] T.-Y. Lin, P. Goyal, R. Girshick, K. He, P. Dollár, Focal Loss for Dense Object Detection, in: *Proceedings of the IEEE/CVF Conference on Computer Vision (ICCV)*, 2017, pp. 2980–2988.
- [32] J. Opitz, S. Burst, Macro f1 and Macro f1, *arXiv preprint arXiv:1911.03347* (2019).
- [33] S. M. Vieira, U. Kaymak, J. M. Sousa, Cohen’s Kappa Coefficient as a Performance Measure for Feature Selection, in: *International Conference on Fuzzy Systems*, IEEE, 2010, pp. 1–8.
- [34] M. Tan, Q. Le, EfficientNet: Rethinking Model Scaling for CNN, in: *International Conference on Machine Learning (ICML)*, 2019, pp. 6105–6114.
- [35] K. He, X. Zhang, S. Ren, J. Sun, Deep Residual Learning for Image Recognition, in: *Proceedings of the IEEE/CVF Conference on Computer Vision and Pattern Recognition (CVPR)*, pp. 770–778.
- [36] C. Szegedy, W. Liu, Y. Jia, P. Sermanet, S. Reed, D. Anguelov, D. Erhan, V. Vanhoucke, A. Rabinovich, Going Deeper with Convolutions, in: *Proceedings of the IEEE/CVF conference on Computer Vision and Pattern Recognition (CVPR)*, 2015, pp. 1–9.
- [37] A. G. Howard, M. Zhu, B. Chen, D. Kalenichenko, W. Wang, T. Weyand, M. Andreetto, H. Adam, MobileNets: Efficient Convolutional Neural Networks for Mobile Vision Applications, *arXiv preprint arXiv:1704.04861* Accessed on 30.01.2022 (2017).
- [38] G. Huang, Z. Liu, L. Van Der Maaten, K. Q. Weinberger, Densely Connected Convolutional Networks, in: *Proceedings of the IEEE/CVF conference on Computer Vision and Pattern Recognition (CVPR)*, 2017, pp. 4700–4708.